AD-E 300092

⑫

DNA 4407T

ADA050703

ASSESSMENT OF CABLE RESPONSE SENSITIVITY TO CABLE AND SOURCE PARAMETERS IN LOW FLUENCE X-RAY ENVIRONMENTS

TRW Defense & Space Systems Group

One Space Park

Redondo Beach, California 90278

8 April 1977

Topical Report for Period January 1977—April 1977

CONTRACT No. DNA 001-77-C-0084

APPROVED FOR PUBLIC RELEASE;
DISTRIBUTION UNLIMITED.

DDC

RECEIVED

MAR 2 1978

B

Prepared for

Director

DEFENSE NUCLEAR AGENCY

Washington, D. C. 20305

DDC FILE COPY

REPORT DOCUMENTATION PAGE		READ INSTRUCTIONS BEFORE COMPLETING FORM
1. REPORT NUMBER DNA 4407T	2. GOVT ACCESSION NO.	3. RECIPIENT'S CATALOG NUMBER
4. TITLE *(and Subtitle)* ASSESSMENT OF CABLE RESPONSE SENSITIVITY TO CABLE AND SOURCE PARAMETERS IN LOW FLUENCE X-RAY ENVIRONMENTS.		5. TYPE OF REPORT & PERIOD COVERED Topical Report for Period Jan — Apr 77
		6. PERFORMING ORG. REPORT NUMBER
7. AUTHOR(s) David M./Clement Charles E./Wuller		8. CONTRACT OR GRANT NUMBER(s) DNA 001-77-C-0084
9. PERFORMING ORGANIZATION NAME AND ADDRESS TRW Defense & Space Systems Group One Space Park Redondo Beach, California 90278		10. PROGRAM ELEMENT, PROJECT, TASK AREA & WORK UNIT NUMBERS Subtask R99QAXEE503-07
11. CONTROLLING OFFICE NAME AND ADDRESS Director Defense Nuclear Agency Washington, D.C. 20305		12. REPORT DATE 8 Apr 77
		13. NUMBER OF PAGES 42
14. MONITORING AGENCY NAME & ADDRESS*(if different from Controlling Office)*		15. SECURITY CLASS *(of this report)* UNCLASSIFIED
		15a. DECLASSIFICATION/DOWNGRADING SCHEDULE

16. DISTRIBUTION STATEMENT *(of this Report)*

Approved for public release; distribution unlimited.

17. DISTRIBUTION STATEMENT *(of the abstract entered in Block 20, if different from Report)*

18. SUPPLEMENTARY NOTES

This work sponsored by the Defense Nuclear Agency under RDT&E RMSS Code
B323077464 R99QAXEE50307 H2590D.

19. KEY WORDS *(Continue on reverse side if necessary and identify by block number)*
Cables
X-Ray Response
Photon Source Sensitivity
Cable Parameter Sensitivity

20. ABSTRACT *(Continue on reverse side if necessary and identify by block number)*

The direct injection response of satellite cables to low fluence X-Ray
environments has been analyzed with respect to certain cable parameters and
photon source parameters. Cable parameters considered were the following:
conductor materials, conductor flashing, number of conductors, gap sizes,
shield thickness, dielectric material, cable size, characteristic impedance,
cable type, and cable loads. Source parameters considered were spectra and
angle of incidence. The most sensitive cable parameter was gap size. It was

DD FORM 1473 EDITION OF 1 NOV 65 IS OBSOLETE
1 JAN 73

409 637

20.   ABSTRACT (Continued)

cont. ▷found that cable response was fairly insensitive to black-body spectra, at
least within the ranges of black-body spectra considered.

CONTENTS

ACCESSION for

NTIS	White Section ■
DDC	Buff Section ☐
UNANNOUNCED	☐
JUSTIFICATION	

BY
DISTRIBUTION/AVAILABILITY CODES

| Dist. | AVAIL. and/or | SPECIAL |
| A | | |

1

FIGURES

TABLES

1.0 INTRODUCTION

For satellite designs which employ RF shielded cables as signal and secondary power lines, and which provide at least 40 dB shielding, the dominant SGEMP mechanism from an exoatmospheric nuclear event is from the direct interaction of incident X-ray photons with the cables themselves. The basic phenomenology is simply that electrons, which are ejected from cable conducting surfaces including the shield, stimulate the flow of replacement current directly on the cables' center wire(s). In this section we give a brief review of the phenomenology and experiments which form the basis of our present understanding of the direct injection response of shielded cables.

In several respects the direct injection response of cables is simpler to treat than, say, the problem of calculating skin currents on a satellite, or fields inside a satellite cavity. For one thing, the cable diameter tends to be much smaller than the dominant wavelengths of the pulse, and it is therefore reasonable to replace Maxwell's equations by their quasistatic counterparts. Secondly, the transport of electrons in dielectrics is not influenced by the generated fields, at least for X-ray fluences relevant to satellites, and it is not necessary to self-consistently calculate the motion of the electrons. It is true that in contrast to other SGEMP mechanisms one might have to worry about radiation induced dielectric conductivity of a cable's insulation, but again one finds that for fluences relevant to satellites, the induced conductivity has slight effect. Finally, the direct injection mechanism leads immediately to a set of current drivers which can be used immediately in transmission line equations to determine load response. For satellite skin currents, in contrast, it is a much more difficult problem to estimate the induced load response to a given threat, and the calculations are clearly more uncertain.

The net result of the simplifications mentioned above is that the problem of determining a satellite's cable response to X-ray photons divides naturally into three parts:

1) determine the deposition of charge in cable dielectrics (solve the electron-photon transport problem)

2) determine the induced current (solve for the Norton-equivalent drivers)

3) determine the response of cable loads, i.e., peak power and energy (solve the transmission line equations)

Concerning the first point, charge deposition and electron-photon transport for photon energies varying from 1 to 300 keV, the exponential photon attenuation of X-rays is generally accepted. For cables the charge deposition profiles are obtained either from analytic treatments such as that of Dellin and MacCallum who solve the Spencer-Lewis transport using certain approximations, or simplified

Monte-Carlo treatments such as SAI's POEM code. A comparison of the different transport code results is given in Figure 1-1 for SANDYL, QUICKE2 (Dellin-MacCallum), and POEM. The main point is that the codes differ from one another on the order of 25% at most. In addition, the comparison between analytic (Dellin-MacCallum), Monte Carlo (SANDYL) and experimental electron energy and angular distributions is quite good.[1]

The solution to finding the induced current once the charge deposition was known was sketched by Van Lint for coaxial cables[2] and was generalized to shielded multi-conductor cables by Clement, et al[3] and Chadsey, et al.[4] Essentially one applies Green's reciprocation theorem which states, for example, that a charge Q, driven from a coax cable shield, will give rise to an image charge $-Q\psi(\vec{r})$ on the shield where $\vec{r}$ is the point where the electron stops in the dielectric, and $\psi(\vec{r})$ is the Laplace equation solution with unit potential on the center wire. Implicit here is the assumption of TEM propagation for lossless lines, i.e., E-fields are normal to the cable axis, and for each element of length along the axis, the currents sum to zero for all the conductors including the shield. These conditions may be relaxed slightly to allow for lossy lines, and a quasi-TEM propagation results.[5]

The final problem, namely, the transmission line solution of either cable bundles or coax cables, with SGEMP direct injection drivers, has not been given much attention, though some preliminary work has been performed by L. E. Shaw and T. J. Sheppard.[6]

So far we have confined ourselves to a discussion of the phenomenology and analyses. Concerning the experimental testing of cables in X-ray environments the pioneering work was done by Fitzwilson and Bernstein.[7] They irradiated small samples of cable in the Aerospace Dense Plasma Focus (DPF) which is (roughly) a filtered 15 keV blackbody source, and compared the experimental results with analytic results generated by the TRW PICS code. The agreement between analyses and experiment was usually better than a factor of two, but the most interesting result was the identification of the importance of gaps separating conductors, particularly shield conductors, from dielectric insulation. These gaps, which are mostly unintentional, give electrons a free ride, thus increasing the electrons' displacements, and since an electron range at these energies is less than the gap size, the amount of image current generated depends critically on the gap size. Since Fitzwilson's paper, Aerospace (Hai, et.al.[8]) has extended its work to testing semi-rigid cables, with favorable comparisons with TRW's MCCABE code (a multi-conductor generalization of the PICS code mentioned above[3]). Aerospace has also summarized all of its results of the DPF testing of cables in a concise report.[9]
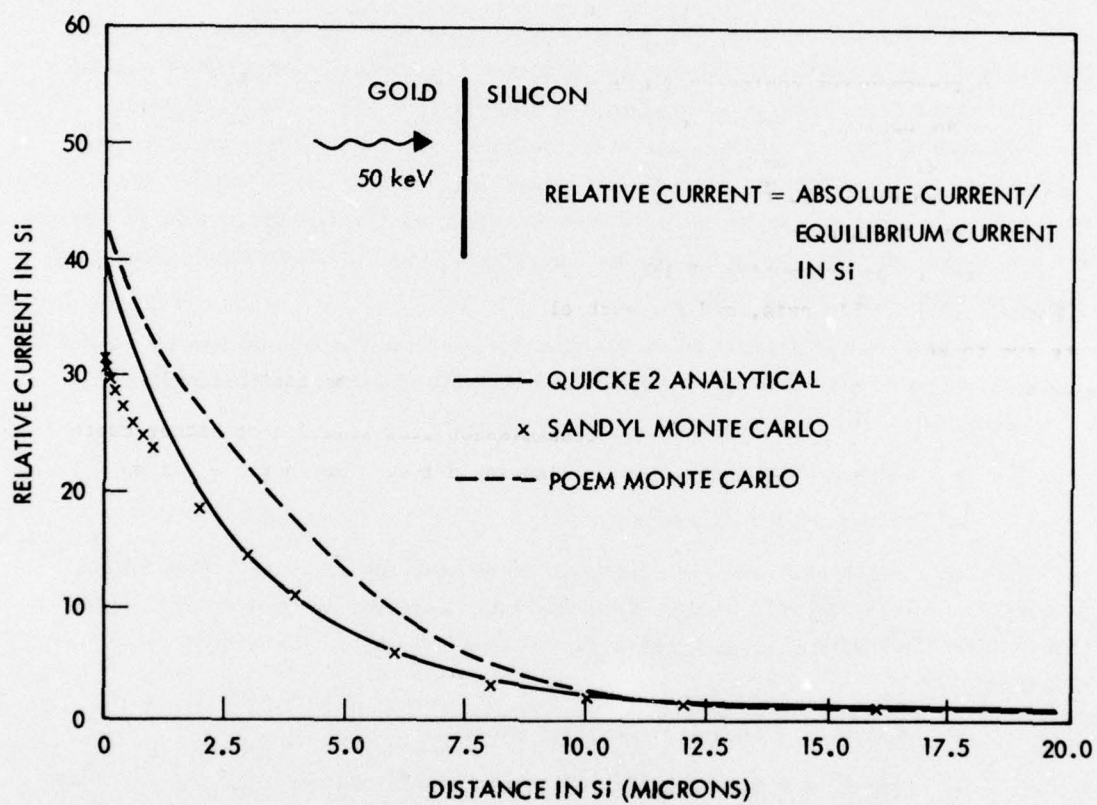
Figure 1-1. Comparison of Electron-Photon Transport Calculations

The experimental efforts mentioned above measured the common-mode current, rather than the individual wire current, even though some of the cables were multi-conductor. In order to verify our multi-conductor cable model which is capable of predicting individual wire currents, we conducted tests at the Simulation Physics facilities on specially prepared multiconductor cables.[3] The agreement between measured and predicted results was quite good, and constitutes at least a partial verification of the MCCABE code.

At this point, then, we can say there is a small but growing body of information on the X-radiation testing and analyses of shielded cables, both coaxial and multi-conductor. So far as analysis is concerned, we have some confidence that our methodology is correct, and that the basic physical mechanisms have been identified, at least for the response of cables in vacuum at low fluence. Concerning the experimentation on cables, we know that a number of low fluence photon simulators are available, we know how to design and instrument a set of cable experiments, and obtain results in a useful form.

Since we now believe we understand the basic mechanisms governing cable response, we are in a position to perform sensitivity studies on direct injection cable response. In other words, we can now vary both

- cable parameters

- photon source parameters

to investigate which ones are most critical in determining response. That is the principal objective of this study. From the data generated in this study we would hope to provide answers, or at least a set of suggestions, to accomplish the following:

- design of a hardened satellite cable

- determine the suitability of photon simulators for
  cable and cable harness testing

The results of the sensitivity assessments and our conclusions are presented in Section 3.0, but before doing this, we give a detailed discussion of the principal output of the assessments, namely the normalized current drivers. This is done in Section 2.0. The purpose is to make sure that these drivers are interpreted properly, and that their connection with transmission line equations on the one hand, and experimental measurements on the other, are clear.

Finally, in Section 4.0 we present a simple rule of thumb for determining the normalized response of coaxial cables.

The assumptions under which these assessments are generated are

- the cables are in vacuum

- the fluence is low enough that limiting effects are unimportant

The tool employed to generate the response sensitivity data is the MCCABE code, the details of which have been described in reference 3.

2.0 DEFINITION OF THE DIRECT INJECTION SOURCE TERMS

2.1 Equivalent Circuit Model for Lossless Lines

Consider a cross section of a shielded multi-wire cable, as shown in the Figure 2-1 (a).
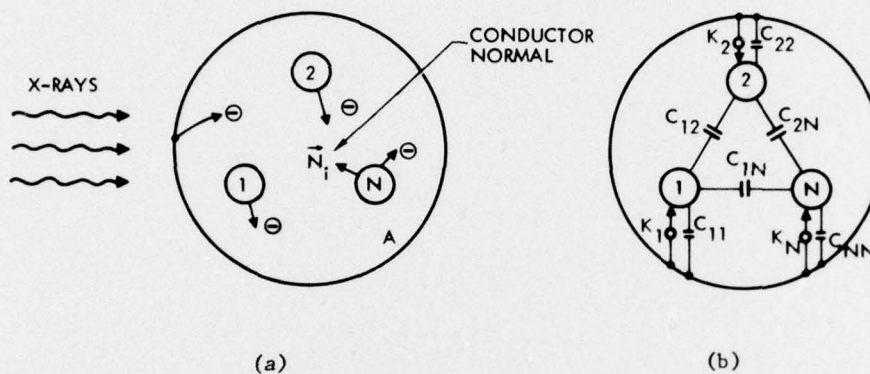
Figure 2-1. (a) Phenomenology of X-radiation Response
of Cables; (b) Equivalent Circuit
Model and Norton Equivalent Drivers

The effect of X-irradiation is to drive electrons from conducting surfaces and deposit them in surrounding dielectric materials, thus stimulating the flow of replacement current. The equivalent circuit model which describes both the phenomenology of electron deposition and conductor currents and voltages, is shown in Figure 2-1 (b). The conditions under which this equivalent model are valid are as follows:

1) the electric field is derivable from a scalar potenital, i.e., TEM propagation;

2) the electron transport is not field (voltage) limited;

3) insulation conductivity may be ignored, including radiation-induced conductivity.

The basic elements of the model include N Norton equivalent drivers K_1 (in units of current per unit length), and $N(N+1)/2$ capacitances (capacitance/per unit length). The simplest form in which to represent the drivers K_1 is

$$K_i = \int_A d^2r \frac{\partial \rho}{\partial t} \psi_i(\vec{r}) \qquad (2\text{-}1)$$

where

> A = total area enclosed by shield (including inner conductors)
>
> $\frac{\partial \rho}{\partial t}$ = rate of volume charge deposition
>
> $\psi_i(\vec{r})$ = solution of 2 dimensional Laplace equation with unit
>   potential on conductor i, all others grounded

If the point $\vec{r}$ is inside any of the interior conductors j, then $\psi_i(\vec{r})$ is δ_{ij}
by definition. These drivers K_i represent source terms in the lossless transmission
line equations,

$$\frac{dI}{dx} = -i\omega C'V + K \qquad (2\text{-}2)$$

$$\frac{dV}{dx} = -i\omega LI$$

where all quantities are in the frequency domain and represent vectors or
matrices of dimension N, the total number of inner wires in the multiwire model,
and where

> ω = $2\pi f$
>
> C' = capacitance matrix defined by $Q = C'V$
>
> LC' = v^{-2}
>
> v = cable propagation velocity, common mode

The equations would then be solved with the boundary conditions that the ratio of
current to voltage at each end of the line is given by the appropriate admittance
matrix element. If the loads themselves are dynamic (i.e., either time or voltage
dependent), then the transmission line equations are solved in the time domain.

A limiting case of interest is the short-circuit current, or more
precisely, one end of the cable is open, the other is short. Then one can show
that for a length of cable $D << \lambda$, where λ represents the dominant wavelengths
of the driving X-ray pulse,

$$I_{sc} = KD$$

This identifies the Norton driver K_i as the short-circuit current per unit length, or
the individual wire current flowing to ground through a low impedance load. In other
words the K_i can be measured directly.

9

For fluences of interest to satellites the driver K is directly proportional to flux. Therefore, it is customary, when measuring or calculating K, to normalize it to the peak flux or peak dose rate. The former is more convenient for extrapolating to defined environments; the latter is more convenient for measurements where the dose rate is obtained directly from photo-diodes.

2.2 The MCCABE Code

We discuss in more detail the current drivers K_i and their relation to the quantities calculated in the MCCABE code. First, we divide the integration area in eq. (2-1) into two parts: the dielectric area and the conducting areas and apply the divergence theorem to the second term, after $d\rho/dt$ has been replaced by $-\vec{\nabla} \cdot \vec{J}$, obtaining

$$K_i = \int_D d^2 r \, \frac{\partial \rho}{dt} \, \psi_i(\vec{r}) \, - \int_{C_i} dl_i \, \vec{J} \cdot \vec{n}_i \tag{2-3}$$

Here the contour C_i refers to the ith conductor's perimeter, and $\vec{n}_i$ is the normal directed out of the conductor i. Next, we note that the current density $\vec{J}(\vec{r})$, falls two to three orders of magnitude as the observation point moves an electron range from the conductor into the bulk. Setting the bulk dielectric current to zero, we take the current density at the interface and treat it as a "yield" or "emission" from conductor j which is to be deposited at discrete points $\vec{r}(j)$. Then, in this formalism

$$\int_D d^2 r \, \frac{\partial \rho}{dt} \, \cdots = \sum_{j=0}^{N} \, \sum_{\vec{r}(j)} \, J_{dep} (\vec{r}(j)) \, \cdots \tag{2-4}$$

where $J_{dep} (\vec{r}(j))$ is the charge/length deposited at the point $\vec{r}(j)$, having originated from conductor j. (The conductor j=0 is the shield). But the total charge emitted from conductor j is the current density at the interface, integrated about the emitting surface

$$\oint_{C_j} \vec{J} \cdot \vec{n}_j \, dl_j = \sum_{\vec{r}(j)} \, J_{dep} (\vec{r}(j)) \tag{2-5}$$

Inserting (2-4) and (2-5) into (2-3) we obtain for the current driver K_i

$$K_i = \sum_{j=0}^{N} \sum_{\vec{r}(j)} J_{dep}(\vec{r}(j)) \begin{cases} \psi_j(\vec{r}(j)), & j \neq i \\ \psi_j(\vec{r}(j)) - 1, & j = i \end{cases} \qquad (2-6)$$

The phenomenology developed to calculate eq. (2-6) is described in detail in reference 3, and is incorporated into the MCCABE code. No change has been made in the code (with one exception: the ability to treat conductor flashing thickness, cf Section 3), and it is not necessary to repeat the formalism here. Basically the code calculates J_{dep} using the formalism of Dellin and MacCallum, where electrons are emitted from a conductor with a specified energy and angular distribution. They cross gaps, where they exist, and penetrate dielectric insulation. The Laplace solution in eq. (2-6) is obtained from a circular harmonic expansion of the integral solution to the Laplace equation, followed by a matrix inversion to obtain the expansion coefficients.

3.0 ASSESSMENT OF CABLE RESPONSE SENSITIVITY

3.1 General Approach

The objectives of this assessment are two-fold. First we want to find out what cable parameters are critical in determining the direct injection response of cables. This information would be useful in designing a cable to minimize direct injection cable response. Secondly, we want to see how the direct injection response depends on photon source characteristics. This will enable one to decide on the suitability of photon simulators relative to nuclear weapons characteristics for testing cables and cable bundles.

Concerning the first point, cable parameter sensitivity, these parameters are the following:

- conductor materials
- conductor flashing
- number of conductors
- gap sizes, between dielectric insulation and conductors
- shield thickness
- dielectric material
- cable size
- characteristic impedance
- cable type
- cable length
- cable loads

These parameters will be discussed in much more detail in the next section. The point we want to make is that the matrix of possible variations to determine sensitivity is considerable. To restrict this range to something manageable there are two possible approaches which we considered. First, one could restrict oneself to a small set of satellite flight-qualified cables and analyze their response. We rejected this approach for two reaons. First, the number of cables in the restricted subset is still impossibly large. And even then, one should realize that cable manufacturers can design a cable to meet almost any specification anyway, and therefore the subset may not ultimately be representative. More important is that several of the above parameters would change in going from cable to cable, making it difficult to see which was the more important in controlling response.

12

The approach which we finally adopted was to define a "standard" 50Ω coaxial cable, and perform single parameter variations from the standard coax of the above parameters. Although this procedure is far from complete (e.g., varying combinations of parameters is of interest) it should give a reasonable indication of what parameters are important in cable response. If one wants to proceed further to designing a hardened cable, one could use these calculations as a starting point for performing more detailed parametric assessments.

Two parameters mentioned above - cable length and cable loads - are not considered in this assessment since they would involve a detailed specification of cable loads, cable harness design, and cable function, and this was out of scope of our defined tasks. Accordingly, we report only the current injected per unit length and flux (the current drivers in Eq. 2-1).

Concerning photon source sensitivity the following parameters are of interest

- fluence
- waveform
- spectrum
- angle of incidence

Of these, fluence and waveform are not considered for the following reasons: we assume that for fluences of interest to satellites the response is linear with flux. (We will address ourselves to the validity of this assumption in a subsequent report). Accordingly, we report only normalized drivers of Eq. (2-1). Concerning waveform variations the drivers themselves follow the X-ray pulse for the same reason. Of course, load response does not necessarily follow the pulse, but we have not addressed this problem.

Spectral variation of photon simulators is of primary concern. At first we thought of using the published spectra of various simulators. However, we concluded that this was impractical for a number of reasons, chief among which was the fact that there are such a large number of such spectra, and even several spectra for the same simulator, depending on how it is operated and/or filtered.

We felt, therefore, that it would be more useful to publish direct injection cable response in two ways: first as a function of monochromatic photon energy, and secondly as a function of blackbody temperature. Concerning the first point, suppose one is presented with an X-ray spectral distribution, $U(E)$ with arbitrary normalization ($U(E) \equiv$ arbitrary unit/keV); then our data may be employed

to find the spectral response via

$$(Response)_{spectrum} = \frac{\int_0^\infty U(E) \ (Response \ (E))_{mono} \ dE}{\int_0^\infty U(E) \ dE}$$

In addition, the presentation of the data as a function of blackbody temperature should be useful in facilitating comparison with nuclear threats. We also remark that our data on the current drivers is valid even if the X-ray spectrum itself is time dependent.

3.2 Units Of Direct Injection Response

In subsequent sections we report the normalized current drivers in units of C-cm/cal, i.e.,

$$\frac{current/length}{flux} = \frac{A/cm}{cal/cm^2-sec} = \frac{C-cm}{cal}$$

This unit is convenient when the threat in cal/cm^2 is specified.

Sometimes it is useful to report the normalized responses in units of C/rad(Si)·cm

$$\frac{current/length}{dose \ rate} = \frac{A/cm}{rad(Si)/sec} = \frac{C}{rad(Si)·cm}$$

This unit is convenient when photodiode measurements of the source fluence are made coincident with the cable response. Conversion factors from cal/cm^2 to rad(Si) are given in Table 3-1 for monochromatic photons as well as blackbody spectra.

Table 3-1. Conversion Factors From Cal/cm^2 to rad(Si)

spectrum (keV)		1 cal/cm^2 is equivalent to
20	mono	1.7×10^6 rad(Si)
30	"	4.8×10^5 "
50	"	1.0×10^5 "
75	"	3.7×10^4 "
100	"	1.9×10^4 "

14

Table 3-1. Conversion Factors from Cal/cm^2 to rad(Si) (Contd)

spectrum (keV)	1 cal/cm^2 is equivalent to
150 mono	1.3 x 10^4 rad(Si)
5.0 blackbody	1.1 x 10^6 "
7.5 "	7.9 x 10^5 "
10.0 "	5.4 x 10^5 "
12.5 "	3.8 x 10^5 "
15.0 "	2.8 x 10^5 "

3.3 Effects of Single Parameter Variation on Cable Response

3.3.1 Direct Injection Response of the Standard Coax

A standard 50Ω coaxial cable was defined in such a way as to represent a reasonable choice for a satellite flight-qualified cable. We do not mean to imply that this choice somehow represents an optimum choice of a cable, either in terms of its normal operation, or its direct injection response. Its physical parameters are defined in Table 3-2. These parameters also represent the basic input to the MCCABE code.

The response of this cable is plotted in Fig. (3-1) in units of C-cm/cal. Note the minus signs indicate the response is negative. The response is seen to be only mildly dependent on black-body temperature.

Table 3-2. Standard 50Ω Coax Parameters

Materials

        shield = tinned copper
        core = silvered copper
        core insulation = teflon

Dimensions (cm)

        shield thickness = 0.01
        shield inner radius = 0.1
        shield gap width = 0.005

        center conductor radius = .0299
        center conductor gap width = 0.001
        shield flashing thickness = 0.0002
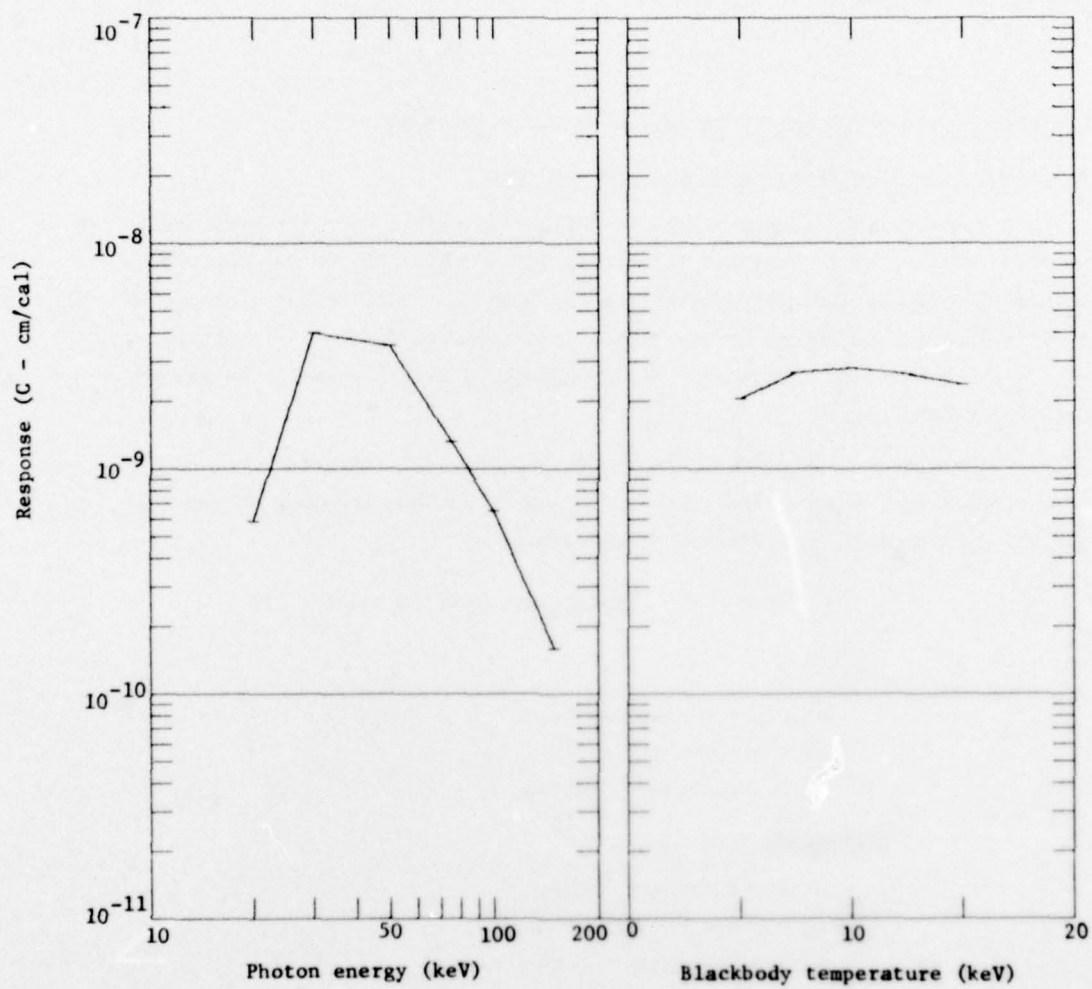   center conductor flashing thickness = 0.0002

Figure 3-1. Direct Injection Response of the Standard Coax

16

3.3.2 Direct Injection Response As A Function of Conductor Materials

In this section we discuss the response of a standard coaxial cable as a function of conductor materials.

The assumption is that the conductor is uniform, and has no flashing. (Flashing variations are discussed in the next section). The following possibilities for conductor materials are felt to be reasonable for satellite cables:

- aluminum (Z = 13)
- copper (Z = 29)
- nickel (Z = 28)
- silver (Z = 47)
- tin (Z = 50)

Each has certain advantages or disadvantages relative to operating temperature requirements for satellites, and ease of making terminations. As far as direct injection response itself is concerned, the smaller the atomic number of both conductors, the smaller the response. Failing that, if one matches the Z's of shield and conductor core, one can have both shield and center conductor buck one another to reduce response.

Results for the standard coax are shown in Figure 3-2. The combinations considered are

	shield	core
1.	aluminum	aluminum
2.	aluminum	copper
3.	copper ($\simeq$ nickel)	copper ($\simeq$ nickel)
4.	silver ($\simeq$ tin)	silver ($\simeq$ tin)
5.	copper ($\simeq$ nickel)	silver ($\simeq$ tin)

As expected, the aluminum-aluminum coax had the lowest response, but even here the lowest response for the 15 keV blackbody spectrum, namely 4×10^{-10} C-cm/cal, is only a factor of 5 lower than the copper-copper cable. Note also that if one replaces only the shield with aluminum, the only effect is to change the sign of the response.

3.3.3 Direct Injection Response As A Function Of Flashing Thickness

Copper or copper alloy is most often the conducting material in satellite cables, but it is rarely used without a coating material such as silver, nickel or tin, to protect it against contaminant oxide layers, or to improve solderability. Unfortunately those additional layers involve higher Z materials which emit more
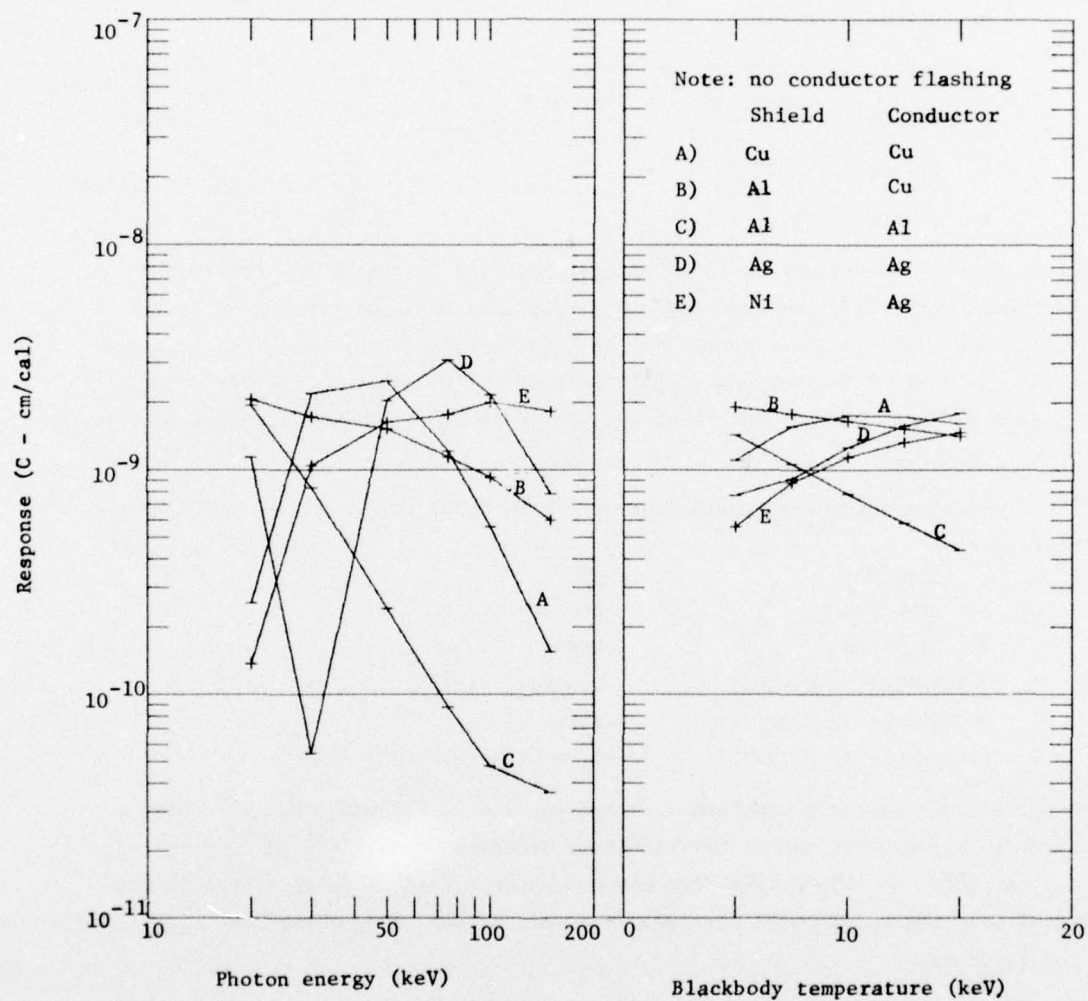
Figure 3-2. Variation of Direct Injection Response With Conductor Materials

electrons, thus increasing the response of the cable.

Now, the use of Dellin-MacCallum emission efficiencies implies that the background material is at least an electron range thick. However, manufacturers quote minimum flashing thicknesses on the order of 40 to 50 microinches, which is the same order of magnitude as an electron range. To remedy the situation we have developed an algorithm, based on the Spencer-Louis transport equation, which replaces the yields from either the bulk or flashing material, by

$$y = y_2^{(\infty)} + (y_1^{(\infty)} - y_2^{(\infty)}) \ (1 - \frac{\rho D}{r}) \ H \ (\bar{r} - \rho D)$$

where

$y_1^{(\infty)}$ = emission efficiency (electrons/photon) from underlying conductor

$y_2^{(\infty)}$ = emission efficiency from conductor flashing

H = step function

ρ = average density of conductors

$\bar{r}$ = average electron range of conductors (g/cm^2)

D = flashing thickness

The expression has the correct limits: (1) for no flashing, $y = y_1^{(\infty)}$; (2) if the flashing is greater than an electron range, then $y = y_2^{(\infty)}$.

In Figure 3-3 we present results for the following conductor-shield combinations

shield	core conductor
bulk conductor - flashing	bulk conductor-flashing
copper-tin	copper-silver
aluminum - (none)	copper-silver
aluminum - (none)	copper

Note that the use of tin flashing is nearly equivalent to silver, and nickel is equivalent to copper, since the Z's are about the same.

Results are shown in Figure 3-3. The amount of flashing thickness used in the standard coax, namely .0002 cm, corresponds to about 80 micro-inches, which is twice the minimum requirements for most satellite cables. After examining photomicrographs of satellite cables, this seemed to be a more realistic number. It is seen from Figure 3-3 that the addition of 0.0002 cm of flashing to copper can increase the response by half an order magnitude.
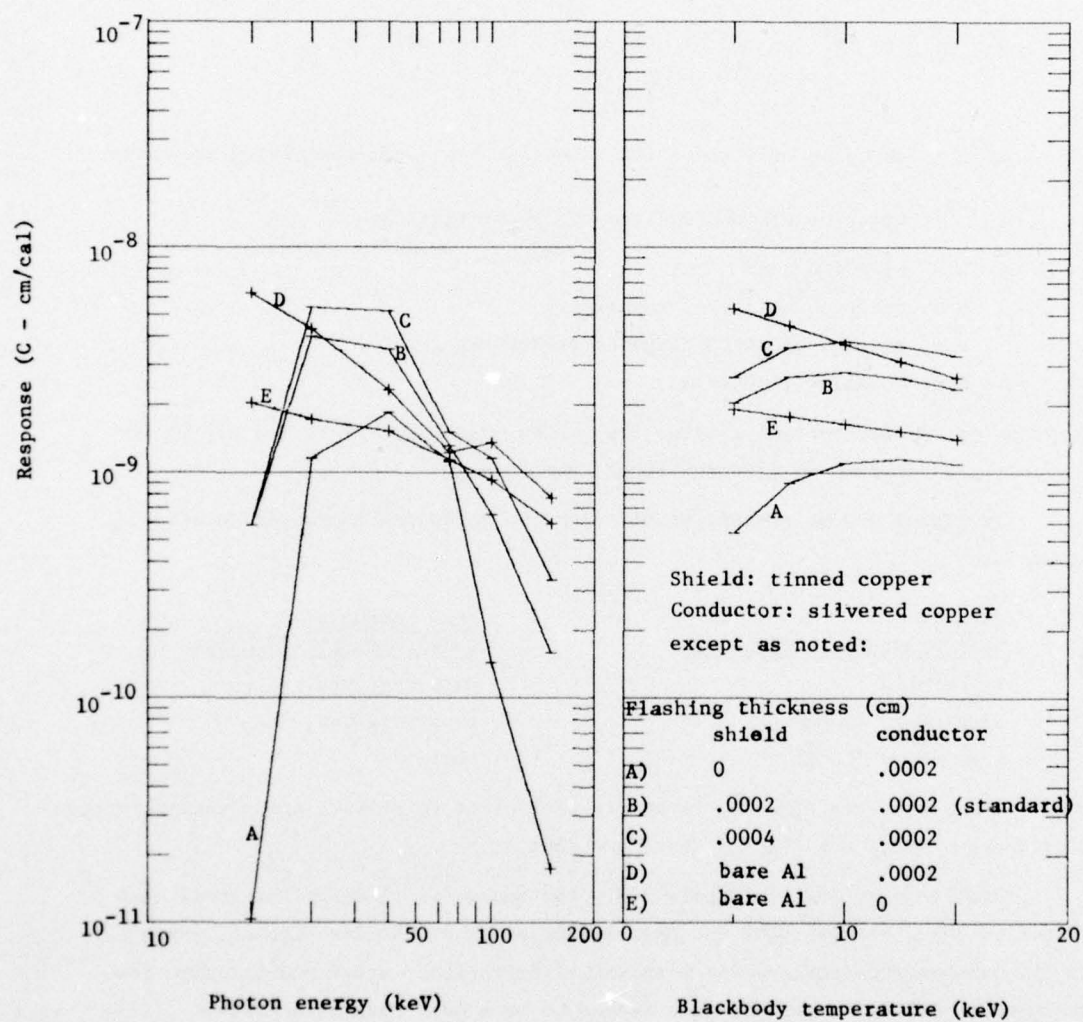
Figure 3-3. Variation of Direct Injection Response With Conductor Flashing Thickness

3.3.4 Direct Injection Response As A Function Of The Number Of Wires In A Cable Bundle

In the calculations which we have performed here we take N insulated conductors whose dimensions are equal to the standard coax center wire (Table 3-2) and close-pack them to form 2- or 4-wire bundles, respectively. Either no-wrap, or single-wrap insulation for the shield is employed whose wrap thickness is the same as the conductor insulation, and this layer is also close-wrapped around the bundle. The shield thickness is the same as for the standard coax.

Results are shown in Figure 3-4. The response of the individual wires of the multiconductor cable tends to be larger than for coaxial cables, not so much because the cable shield is larger, but because a fairly large void exists between the shield and the conductors, even if a shield inner liner is used.

3.3.5 Direct Injection Response As A Function Of Gap Size

In this section we discuss the response as a function of shield gap size and center conductor gap size. Results are presented in Figure 3-5. The size of the gap can affect the response by several orders of magnitude.

For braided cables, the variation in gap size is largely an uncontrolled parameter, depending at least in part on the tightness of the wrap and the size of the individual wire strands. Probably the designation of a gap size in any analytical calculation is only accurate to $\pm 30\%$. Nonetheless, the shield gap size is the most sensitive parameter in determining response. This is because the electrons get essentially a free ride across the gap. Since the gaps in shielded cables tend to be much greater than the range of an electron penetrating a dielectric, the response is amplified accordingly. We would say that braided coaxial cables have gaps on the order of 1 to 3 mil thickness. Solid semi-rigid cables are not supposed to have gaps at all, though in fact we find, after examining photomicrographs that sometimes they do. They tend to be irregular about their circumference, and generally less than 1/10 mil in width. Solid semi-rigids have the smallest direct injection response of all cables.

As far as center conductors are concerned, whether for braided or semi-rigid cables, their gaps tend to be negligible, since the dielectric is usually extruded onto them.

3.3.6 Direct Injection Response As A Function Of Shield Thickness

The results of varying cable shield thickness are shown in Figure 3-6. The effect of the shield is to attenuate the incident X-rays. Shield thicknesses vary significantly depending on whether or not a single or double braided shield is employed. The largest effect occurs at low photon energies where the absorption co-efficients of the conductor material are larger.
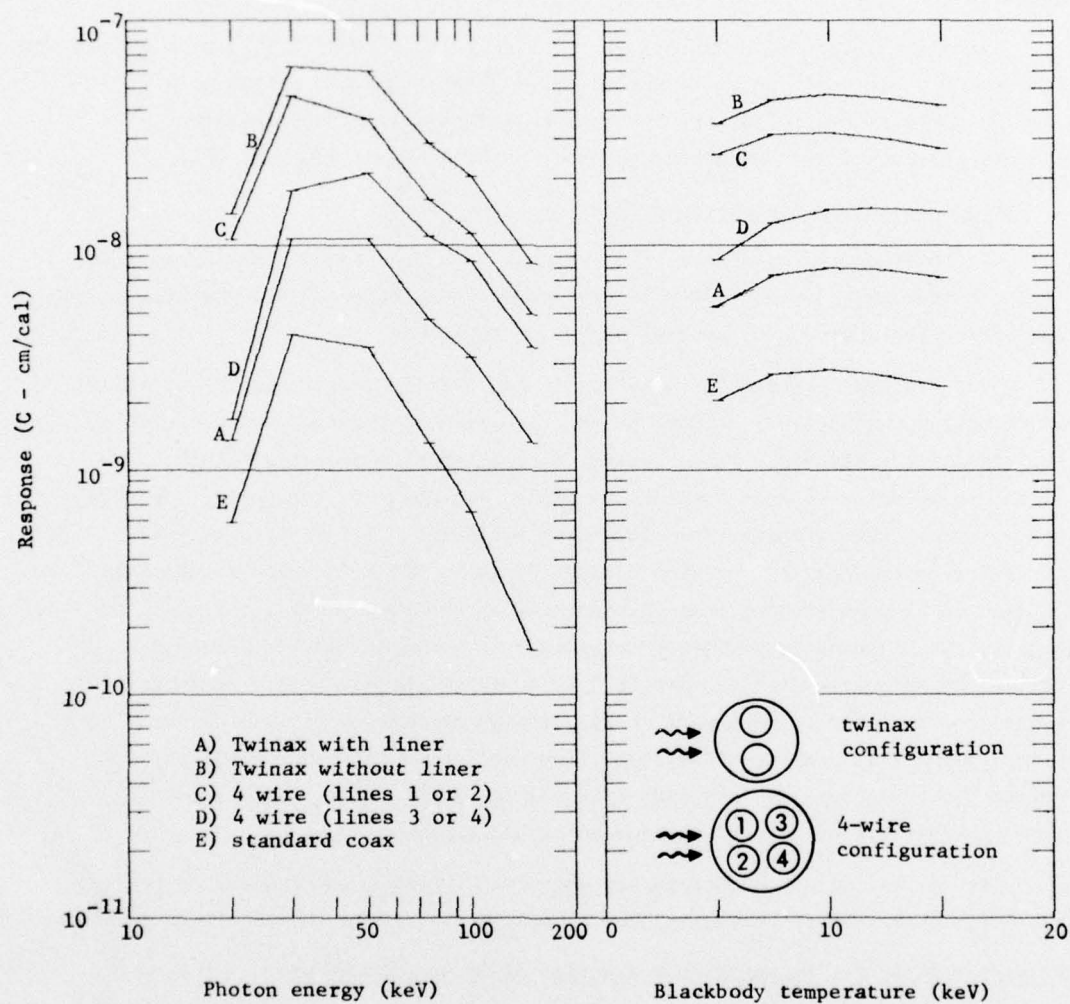
Figure 3-4. Variation of Direct Injection Response With Number of Conductors

22
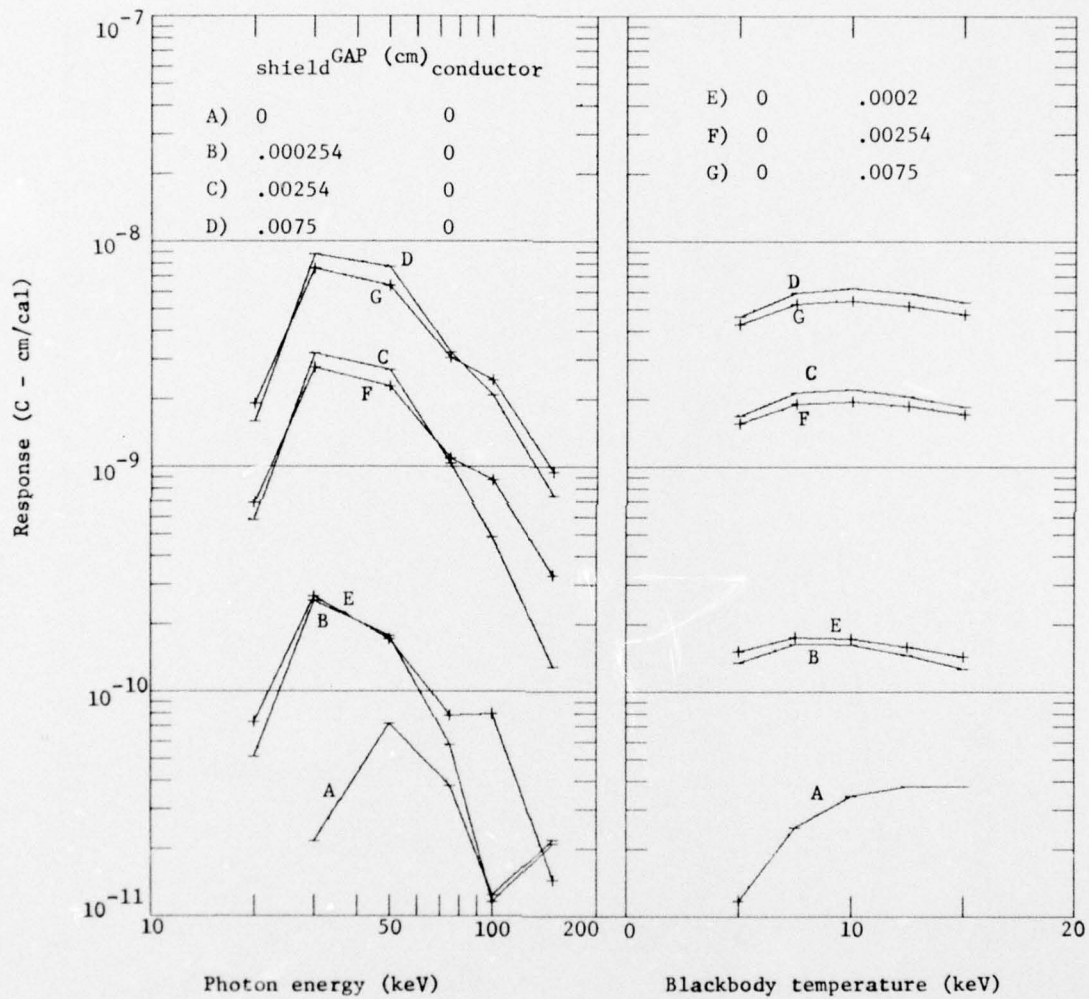
Figure 3-5. Variation of Direct Injection Response With Gap Size

23

10^{-7}

10^{-8}

Response (C – cm/cal)

10^{-9}

A

B

C

D

10^{-10}

A

B

C

D

A) 0

B) .01 cm (standard)

C) .02 cm

D) .04 cm

10^{-11}

10   50   100   200   0   10   20

Photon energy (keV)   Blackbody temperature (keV)

Figure 3-6. Variation of Direct Injection Response With Shield Thickness

3.3.7 Direct Injection Response As A Function Of Dielectric Material

The main effect the dielectric has on the cable response is on the stopping power of electrons which stop in the dielectric insulation, having been emitted from the conductor. Since the stopping power in $MeV/(g/cm^2)$ is nearly independent of the dielectric material, then the range (in cm) is proportional to the density of the insulation. For cables with gaps, however, the electrons get a free ride across the cable gap, and the extra distance traveled in the dielectric is of no consequence. Therefore, one does not expect dielectric insulation to affect response very much. These conclusions are borne out by the results shown in Figure 3-7.

These conclusions may be modified by two considerations which we have not yet examined. (1) If the Z of the dielectric approaches that of the conductors, then the details of the electron transport will affect the response considerably. The present version of the MCCABE code sets the bulk dielectric current to zero and the code will be modified during the next reporting period to handle a bulk dielectric current. (2) The radiation-induced conductivity of the dielectric is ignored. For fluences of interest to satellites, this is of no consequence. A more detailed discussion of this will follow during the next reporting period.

3.3.8 Direct Injection Response As A Function Of Cable Size

In principle the direct injection response is proportional to cable size provided that all dimensions are scaled linearly <u>including gap sizes</u>. This is shown in Figure 3-8. Note that when the gap size is not reduced, the response stays essentially the same. The point is that the outside diameter of a cable is not sufficient to judge its relative direct injection response.

3.3.9 Direct Injection Response As A Function Of Characteristic Impedance

If we choose to vary the ratio of

$$\frac{\text{shield inner diameter}}{\text{conductor diameter}} \equiv \frac{a_o}{a_i}$$

this is equivalent to varying the characteristic impedance Z_o, since it is related to $\frac{a_o}{a_i}$ via

$$Z_o = \frac{59.945 \ln \frac{a_o}{a_i}}{\sqrt{K}} \quad (\Omega)$$

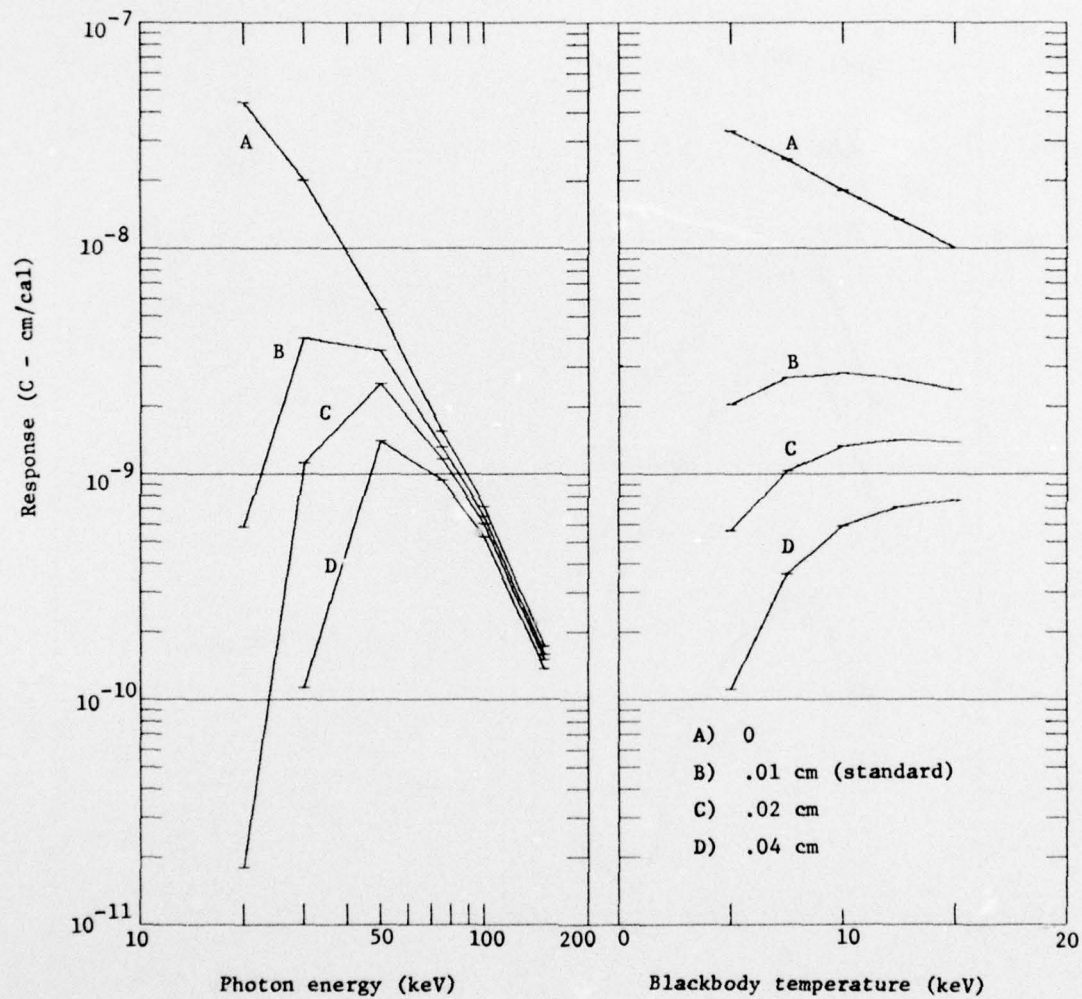where K is the relative dielectric constant of the insulation.

25
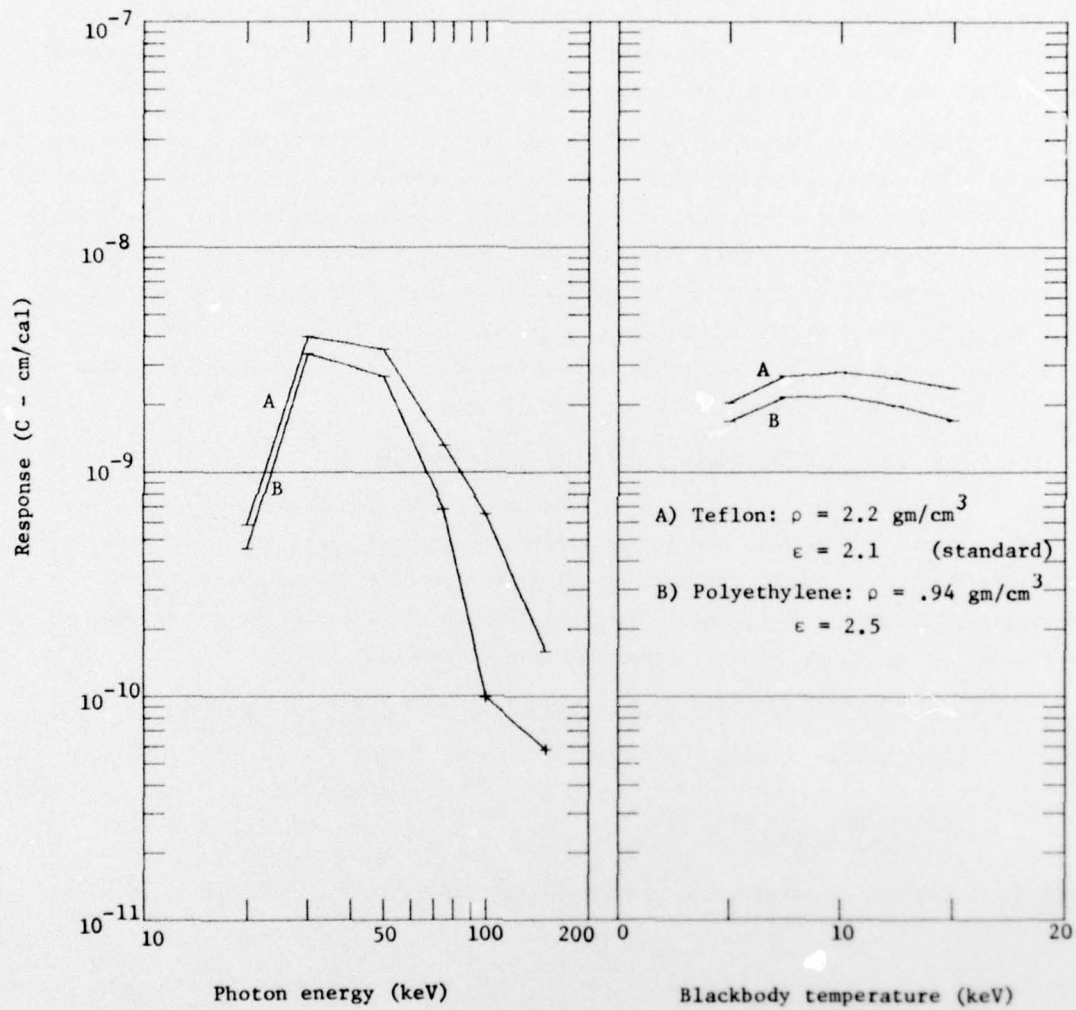
Figure 3-7. Variation of Direct Injection Response With Dielectric Material
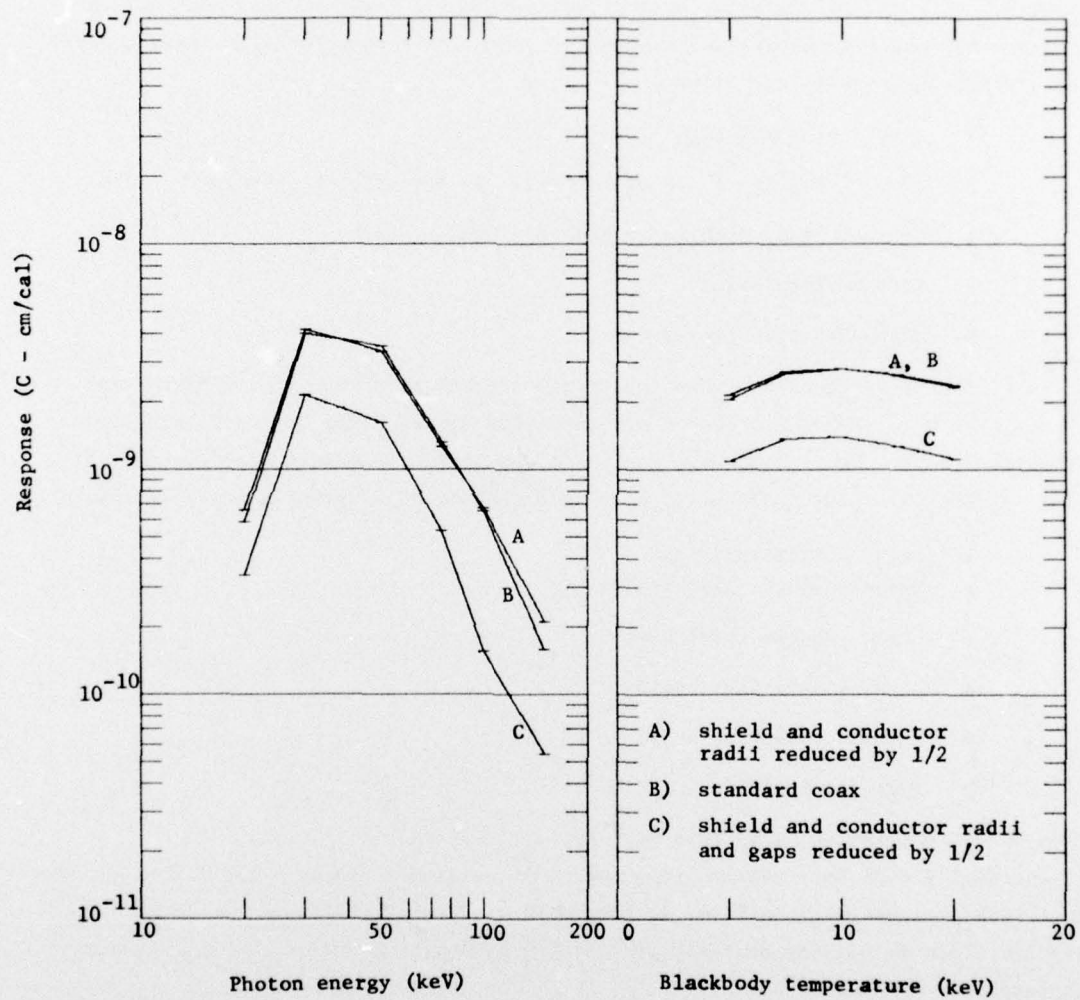
Figure 3-8. Variation of Direct Injection Response With Cable Size

Legend within figure:

A) shield and conductor radii reduced by 1/2

B) standard coax

C) shield and conductor radii and gaps reduced by 1/2

Axis labels: Response (C – cm/cal); Photon energy (keV); Blackbody temperature (keV)

Response as a function of coax characteristic impedance Z_o is presented in Figure 3-9. One can show that the direct injection response is essentially inversely proportioned to $\ln \frac{a_o}{a_i}$ (see section 4.), and this expectation is realized by the data.

3.3.10 Direct Injection Response As A Function Of Cable Type

Cable hardness engineers on satellite programs select cables on the basis of their electrical performance, weight, ease of making terminations, and ability to withstand satellite natural environments. From their point of view, they might classify shielded cables as follows:

- number of conductors: coax or multiwire
- type of shield: braid or solid (as in semi-rigid cables)
- type of braid: single or double, round or flat
- type of insulation
- characteristic impedance

Of these, the first three are more important from the point of view of direct injection response. We have selected six satellite cables based on the first three categories above. The cables were sectioned and their parameters were identified. Their response is shown in Figure 3-10. In the order of decreasing response the cables are:

- coax, hollow semirigid
- twinax, single flat braid
- triax, double round braid
- coax, single flat braid
- coax, double flat braid
- coax, semi-rigid

Based on our previous results this pattern is not difficult to understand: 1) coax cables will have smaller responses than multiwire cables without shield liners since coax gaps are much smaller; 2) the semi-rigid cable will have the least response since it has the smallest gap; 3) the thicker the shield the smaller the response.

3.3.11 Direct Injection Response As A Function Of Azimuthal Angle Of Incidence

The main effect of non-normal angle of incidence on coax response is to increase the path length, and therefore the attenuation of the radiation as it passes through the coax. Response as a function of azimuthal angle ϕ is shown in
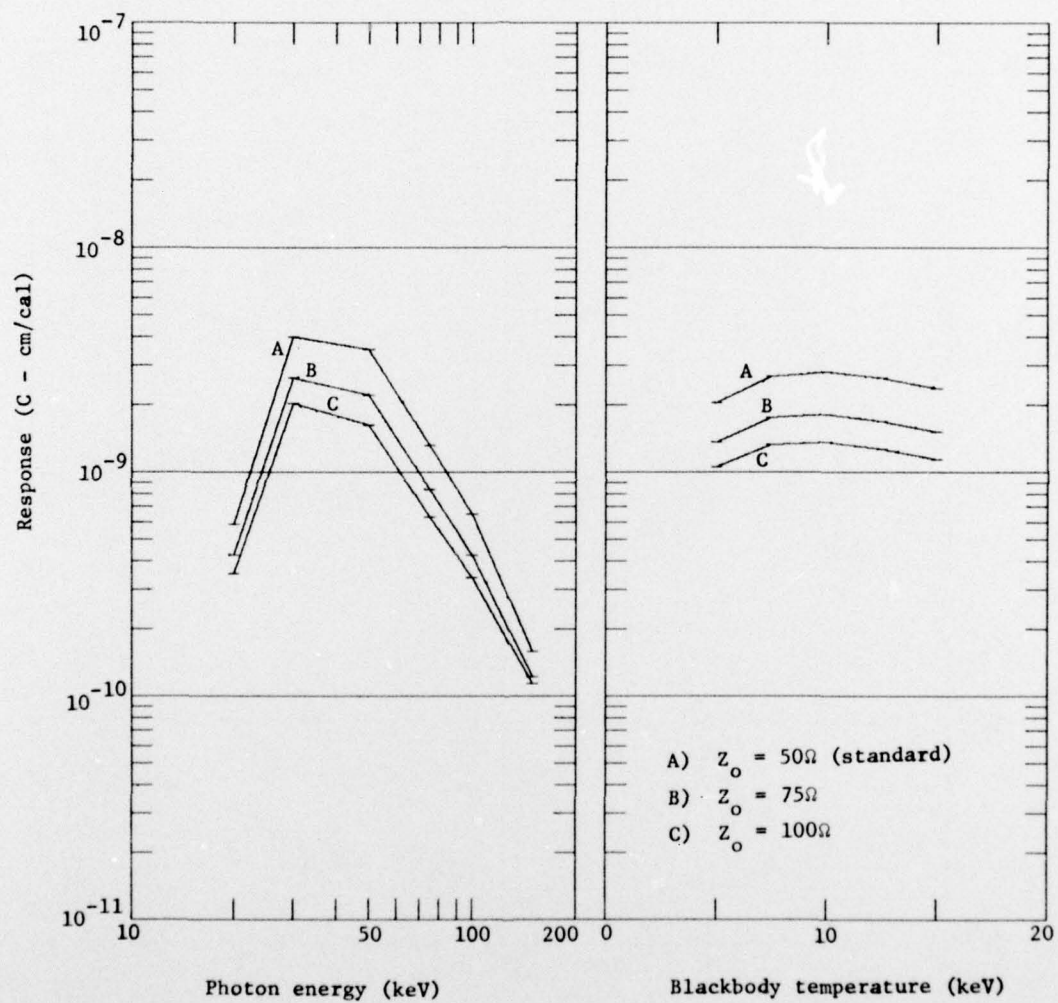
Figure 3-9. Variation of Direct Injection Response With Coax Characteristic Impedance

A) PT3-59-93; coax, double flat braid   D) 3A024-001; semirigid coax (SR086)

B) PT3-33N-22; coax, single flat braid   E) PT3-33P-24; twinax, single flat braid

C) 3A002-006; coax, single flat braid   F) PT3-53RR-18; triax, double round braid

G) 3A024-005; hollow semirigid

Photon energy (keV)   Blackbody temperature (keV)

Figure 3-10. Variation of Direct Injection Response with Cable Type. The Response Is the Common Mode Response per Wire.

Figure 3-11. One concludes that normal incidence is worst case, so far as the drivers are concerned. Whether or not this is true for load response is not clear, since a phase delay in the drivers would have to be introduced in the transmission line solution and "stacking" of the response might occur.

3.4 Conclusions Regarding Cable and Source Parameter Sensitivity

The parameters which produced <u>more than an order of magnitude</u> variation in the direct injection response were

- flashing thickness
- number of conductors
- gap size
- shield thickness
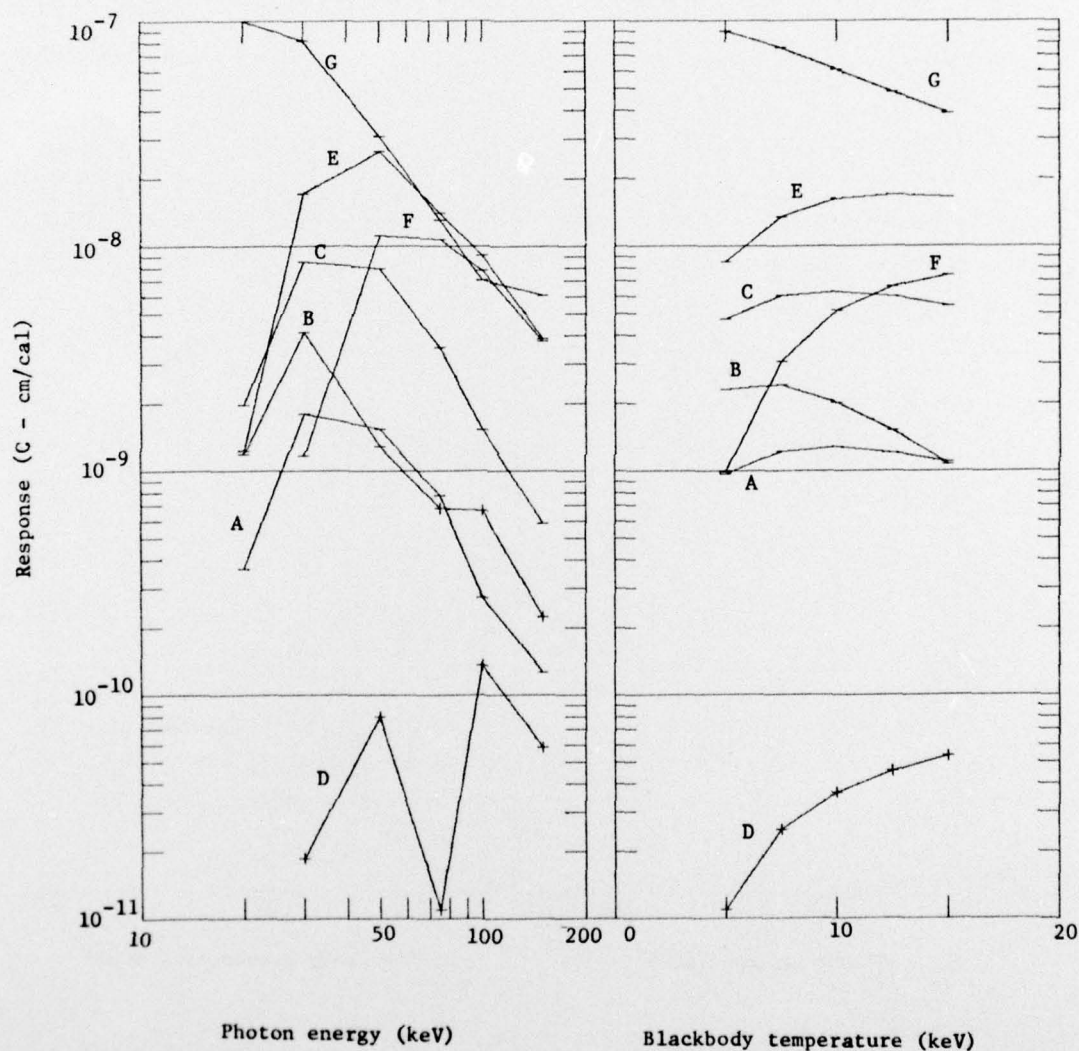- angle of incidence

Of these the gap size produced the most variation.

The parameters which produced <u>less than an order of magnitude</u> variation in the direct injection response were

- conductor material
- dielectric material
- cable size
- characteristic impedance
- spectrum

We realize that the above statement may be misleading since "order-of-magnitude variation" means only that in the range within which we choose to vary parameters, the most significant ones were those indicated. In principle, one could have varied the parameters more drastically to achieve a larger variation of response. We believe, however, that the range over which we varied the parameters is representative of actual satellite cables.

31
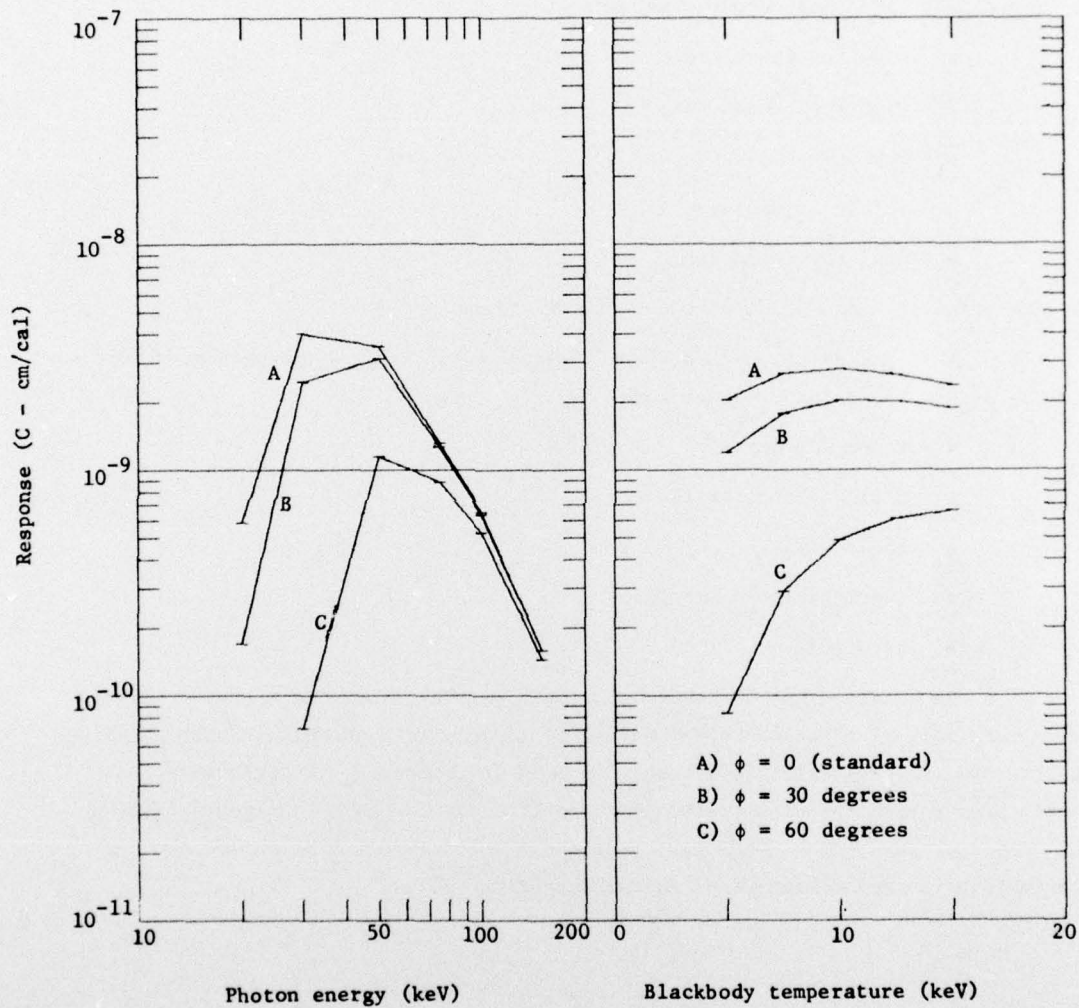
Figure 3-11. Variation of Direct Injection Response With Angle of Incidence

Response (C - cm/cal)

10⁻⁷

10⁻⁸

10⁻⁹

10⁻¹⁰

10⁻¹¹

A

B

C

A) φ = 0 (standard)
B) φ = 30 degrees
C) φ = 60 degrees

10   50   100   200

Photon energy (keV)

0   10   20

Blackbody temperature (keV)

32

4.0 SIMPLIFIED ANALYSIS OF COAXIAL CABLE RESPONSE

We develop here a simple rule of thumb which incorporates most of the physics of cable response as applied to a coaxial cable, but without the details of the exact treatment which the MCCABE code incorporates.

K = dielectric constant

Y_1 = conductor yield

SHIELD

DIELECTRIC

GAPS
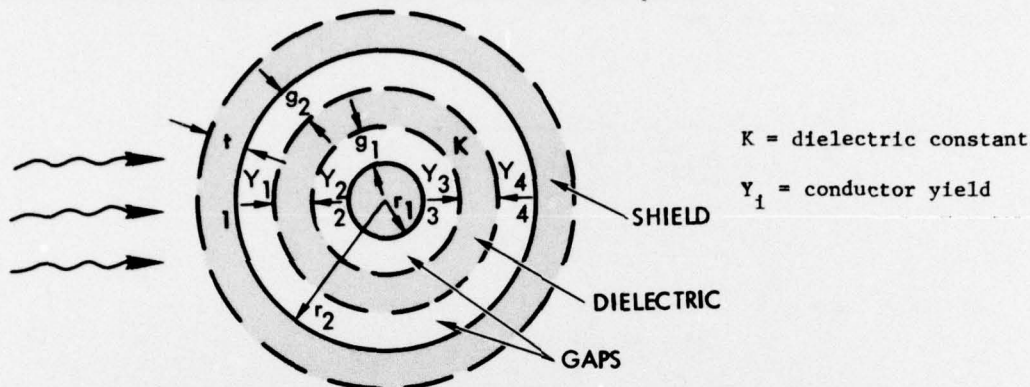
The various geometrical quantities which we need are defined in the figure. The assumptions made are as follows:

A unit flux of 1 cal/cm^2-sec of monochromatic photons of energy E is incident on the cable. At the points 1 through 4 the flux is attenuated by an amount

point 1: $e^{-\mu_s(E)\rho_s t}$

point 2: $e^{-\mu_s(E)\rho_s t}$

point 3: $e^{-2\mu_c(E)\rho_c r_1} e^{-\mu_s(E)\rho_s t}$

point 4: $e^{-2\mu_c(E)\rho_c r_1} e^{-\mu_s(E)\rho_s t}$

where μ_s = absorption coefficient for shield material

ρ_s = density of shield material

μ_c = absorption coefficient for center conductor material

ρ_c = density of center conductor material

At each of the points 1 through 4 the emitted current density is given by

$$\frac{- |e| \; Y(E) \cdot \text{attenuated flux}}{E}$$

where Y(E) is the Dellin-MacCallum forward emission efficiency for the given conductor. The assumption here is that the yield is roughly independent of angle.

33

The total emission current/length is obtained by multiplying the current densities by πr_1 or πr_2 respectively.

The emitted electrons are assumed to cross the gap and stop there. The appropriate Laplace solutions at the point $r = r_2 - g_2$ and $r = r_1 + g_1$, in the limit that g_1/r_1 and $g_2/r_2 \ll 1$ are

$$\psi(r_2 - g_2) = \frac{g_2}{r_2} \quad \frac{1}{(1 - \frac{1}{K})(\frac{g_1}{r_1} + \frac{g_2}{r_2}) + \frac{1}{K} \ln \frac{r_2}{r_1}}$$

$$\psi(r_1 + g_1) - 1 = \frac{-g_1}{r_1} \quad \frac{1}{(1 - \frac{1}{K})(\frac{g_1}{r_1} + \frac{g_2}{r_2}) + \frac{1}{K} \ln \frac{r_2}{r_1}}$$

With these assumptions the short circuit current per unit length per unit flux, in units of C-cm/cal is

$$K \left(\frac{C\text{-}cm}{cal}\right) = \frac{-1.3 \times 10^{-2} \, e^{-\mu_s(E)\rho_s t} \, (Y_s(E) \, g_{2(cm)} - Y_c(E) g_{1(cm)})}{(1 - \frac{1}{K})(\frac{g_1}{r_1} + \frac{g_2}{r_2}) + \frac{1}{K} \ln \frac{r_2}{r_1}} \quad x \quad (4\text{-}1)$$

$$x \quad (1 + e^{-2\mu_c(E)\rho_c r_1}) \, E^{-1} \, (keV)$$

The formula has the virtue of emphasizing the importance of both the emitting materials of each conductor and the gap sizes, through the products (Yg).

As an example we apply this formula to the standard coax whose dimensions were given in Table 3-2. These results are plotted in Figure 4-1. The agreement is quite good, particularly for the blackbody spectra.
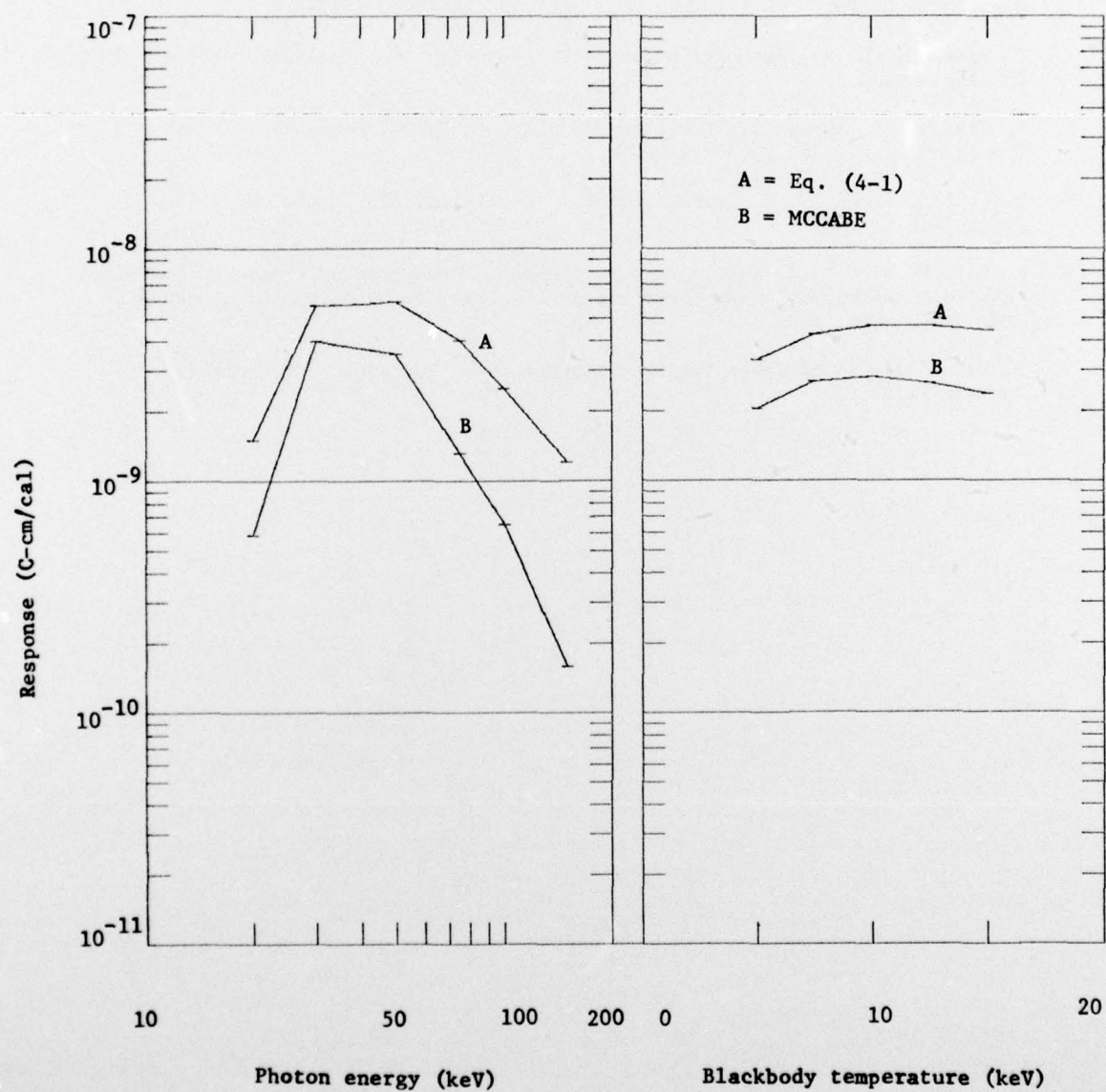
Figure 4-1. Comparison of response of the standard coax using
MCCABE, and a simplified formula, Eq. (4-1)

REFERENCES

1) T. Dellin and C. MacCallum, J. of Applied Physics, v. 46, no. 7, July,
    1975, 2924.

2) V. van Lint, "Radiation-Induced Currents In Coaxial Cables," IEEE Trans.
    Nucl. Sci. NS-17, 210 (1970)

3) D. M. Clement, C. E. Wuller and E. Paul Chivington, "Multiconductor Cable
    Response in X-Ray Environments," IEEE Trans. Nucl. Sci NS-23, 1946 (1976)

4) W. L. Chadsey, B. L. Beers, V. W. Pine, C. W. Wilson, "Radiation-Induced
    Signals in Cables," IEEE Trans. Nucl. Sci. NS-23, 1933 (1976)

5) S. Frankel, "Cable and Multiconductor Transmission Line Analysis," HDL-TR-091-1,
    28 June 1974

6) L. Shaw and T. Sheppard, "Cable Bundle Response In SGEMP Analysis," IEEE
    Trans. Nucl. Sci. NS-23, 1942 (1976)

7) R. L. Fitzwilson, M. J. Bernstein and T. E. Alston, IEEE Trans. Nucl. Sci.
    NS-21, 276 (1974).

8) F. Hai, P. Beemer, C. Wuller, and D. Clement, "Measured and Predicted Radiation-
    Induced Currents In Low Response Coaxial Cables," to be presented at IEEE-NS
    Symposium, July, 1977

9) F. Hai, "Summary of Cable Response Experiments," Aerospace Corporation,
    January 1976.

DISTRIBUTION LIST

DEPARTMENT OF DEFENSE

Director
Defense Communications Agency
        ATTN: NMR

Defense Documentation Center
Cameron Station
12 cy   ATTN: TC

Director
Defense Nuclear Agency
        ATTN: DDST
        ATTN: TISI, Archives
 2 cy   ATTN: RAEV
 3 cy   ATTN: TITL, Tech. Library

Commander
Field Command
Defense Nuclear Agency
        ATTN: FCPR
        ATTN: FCLMC

Director
Interservice Nuclear Weapons School
        ATTN: Document Control

Chief Livermore Division Fld. Command, DNA
Lawrence Livermore Laboratory
        ATTN: FCPRL

National Communications System
Office of the Manager
        ATTN: NCS-TS

Under Secretary of Defense for Rsch. & Engrg.
        ATTN: S&SS (OS)

DEPARTMENT OF THE ARMY

Director
BMD Advanced Tech. Ctr.
Huntsville Office
        ATTN: RDMH-O

Dep. Chief of Staff for Rsch. Dev. & Acq.
        ATTN: DAMA-CSM-N

Commander
Harry Diamond Laboratories
        ATTN: DRXDO-TI, Tech. Library
        ATTN: DRXDO-RCC, John A. Rosado
        ATTN: DRXDO-RCC, Raine Gilbert
        ATTN: DRXDO-NP

Commander
Picatinny Arsenal
        ATTN: SMUPA
        ATTN: SARPA

Commander
Redstone Scientific Information Ctr.
U.S. Army Missile Command
        ATTN: Chief, Documents

DEPARTMENT OF THE ARMY (Continued)

Chief
U.S. Army Communications Sys. Agency
        ATTN: SCCM-AD-SV, Library

Commander
U.S. Army Electronics Command
        ATTN: DRSEL

DEPARTMENT OF THE NAVY

Chief of Naval Research
        ATTN: Henry Mullaney, Code 427

Director
Naval Research Laboratory
        ATTN: Code 5565, P. Ulrich
        ATTN: Code 7750, Jack Davis

Officer-In-Charge
Naval Surface Weapons Center
        ATTN: Code WA501, Navy Nuc. Prgms. Off.

Director
Strategic Systems Project Office
        ATTN: NSP

DEPARTMENT OF THE AIR FORCE

AF Geophysics Laboratory, AFSC
        ATTN: Charles Pike

AF Materials Laboratory, AFSC
        ATTN: Library

AF Weapons Laboratory, AFSC
        ATTN: SUL
 2 cy   ATTN: NTS
 2 cy   ATTN: DYC

Headquarters, USAF/RD
        ATTN: RDQSM

Commander
Rome Air Development Center, AFSC
        ATTN: Edward A. Burke

SAMSO/DY
        ATTN: DYS

SAMSO/MN
        ATTN: MNNG
        ATTN: MNNH

SAMSO/SK
        ATTN: SKF

SAMSO/XR
        ATTN: XRS

Commander In Chief
Strategic Air Command
        ATTN: NRI-STINFO, Library
        ATTN: XPFS

DEPARTMENT OF ENERGY

University of California
Lawrence Livermore Laboratory
        ATTN: Tech. Info. Dept., L-3

Los Alamos Scientific Laboratory
        ATTN: Doc. Control for Reports Library

Sandia Laboratories
Livermore Laboratory
        ATTN: Doc. Control for Theodore A. Dellin

Sandia Laboratories
        ATTN: Doc. Control for 3141, Sandia Rpt. Coll.

OTHER GOVERNMENT AGENCY

NASA
Lewis Research Center
        ATTN: N. J. Stevens
        ATTN: Carolyn Purvis
        ATTN: Library

DEPARTMENT OF DEFENSE CONTRACTORS

Aerospace Corporation
        ATTN: Frank Hai
        ATTN: V. Josephson
        ATTN: Julian Reinheimer
        ATTN: Library

Avco Research & Systems Group
        ATTN: Research Library, A830, Rm. 7201

The Boeing Company
        ATTN: Preston Geren

University of California at San Diego
        ATTN: Sherman De Forest

Computer Sciences Corporation
        ATTN: Alvin T. Schiff

Dr. Eugene P. DePlomb
        ATTN: Eugene P. DePlomb

Dikewood Industries, Inc.
        ATTN: Tech. Library
        ATTN: K. Lee

EG&G, Inc.
Albuquerque Division
        ATTN: Technical Library

Ford Aerospace & Communications Corp.
        ATTN: Donald R. McMorrow, MS G30
        ATTN: Library

General Electric Company
Space Division
Valley Forge Space Center
        ATTN: Joseph C. Peden, VFSC, Rm. 4230M

DEPARTMENT OF DEFENSE CONTRACTORS (Continued)

General Electric Company
TEMPO-Center for Advanced Studies
        ATTN: DASIAC
        ATTN: William McNamara

Hughes Aircraft Company
        ATTN: Tech. Lib.

Hughes Aircraft Company, El Segundo Site
        ATTN: Edward C. Smith, MS A620
        ATTN: William W. Scott, MS A1080

Institute for Defense Analyses
        ATTN: IDA, Librarian

IRT Corporation
        ATTN: Dennis Swift
        ATTN: Technical Library

JAYCOR
        ATTN: Library
        ATTN: Eric P. Wenaas

JAYCOR
        ATTN: Robert Sullivan

Johns Hopkins University
Applied Physics Laboratory
        ATTN: Peter E. Partridge

Kaman Sciences Corporation
        ATTN: Library
        ATTN: W. Foster Rich
        ATTN: Jerry I. Lubell

Lockheed Missiles & Space Co., Inc.
        ATTN: Dept. 85-85

McDonnell Douglas Corporation
        ATTN: Stanley Schneider

Mission Research Corporation
        ATTN: Roger Stettner
        ATTN: Conrad L. Longmire

Mission Research Corporation-San Diego
        ATTN: V. A. J. Van Lint
        ATTN: Library

R & D Associates
        ATTN: Leonard Schlessinger
        ATTN: Technical Library

Rockwell International Corporation
        ATTN: Technical Library

Science Applications, Incorporated
        ATTN: William L. Chadsey

Spire Corporation
        ATTN: Roger G. Little

DEPARTMENT OF DEFENSE CONTRACTORS (Continued)

TRW Defense & Space Sys. Group
        ATTN: Tech. Info. Center/S-1930
        ATTN: David. Clement
        ATTN: Charles E. Wuller
2 cy   ATTN: Robert M. Webb, R1-2410

DEPARTMENT OF DEFENSE CONTRACTORS (Continued)

Systems, Science and Software, Inc.
        ATTN: Andrew R. Wilson
        ATTN: Technical Library